Journal of Stress Analysis
Vol. 4, No. 1, Spring – Summer 2019

Bu-Ali Sina University

Analysis of Bi-directional FG Porous Sandwich Beams in Hygrothermal Environment Resting on Winkler/Pasternak Foundation, Based on the Layerwise Theory and Chebyshev Tau Method

M. Matinfar[a], **M. Mahdavi Shirazi**[a], **M.M. Alipour**[b,*]

[a] Department of Mathematics, University of Mazandaran, Babolsar, Iran.
[b] Department of Mechanical Engineering, University of Mazandaran, Babolsar, Iran.

Article info

Article history:
Received 10 May 2019
Received in revised form
06 July 2019
Accepted 14 August 2019

Keywords:
Chebyshev tau method
Bi-directional functionally graded
Porous sandwich beams
Elastic foundation
Layerwise theory

Abstract

In this paper, for the first time, displacement and stress analysis of bi-directional functionally graded (BDFG) porous sandwich beams are developed using the Chebyshev tau method. Based on the presented approach, sandwich beams under non-uniform load rested on Winkler/Pasternak foundation are analyzed. The material properties of core and each face sheet can be varied continuously in the axial and thickness directions, also the material properties are affected by the variation of temperature and moisture. To overcome some of the shortcomings of the traditional equivalent single layer theories for analysis of sandwich structures, governing equations are extracted based on the layerwise theory and five coupled differential equations are obtained. The resulting differential equations are solved using the Chebyshev tau method (CTM). The effectiveness of the CTM is demonstrated by comparing the obtained results with those extracted from the ABAQUS software. The comparisons indicate that the applied method to solve the systems of ordinary differential equations is efficient and very good accurate.

Nomenclature

$h_i, i = t, c, b$	Thickness of the top, core and bottom face sheets	$u_i, i = t, c, b$	In-plane displacement of the top, core and bottom layers
$f(x)$	Porous distribution in longitudinal direction	$\mathcal{P}_N$	Space of algebraic polynomials of degree at most $N \in \mathbb{N}$, $N > 0$
$\varphi_x^{(i)}, i = t, c, b$	Rotation of the top, core and bottom layers	$\sigma_x^{(i)}, i = t, c, b$	Through the thickness of the in-plane stress
B	Set of linear differential operators defined on -1 and 1	$\alpha^{(i)}$ and $\beta^{(i)}$	Thermal expansion and moisture concentration coefficients
E	Young's modulus	$\delta_{n,m}$	Kronecker delta symbol
X_N	Space of trial or shape functions	$\mathcal{L}$	Linear differential operator
w	Transverse displacement	C	Moisture exposure

*Corresponding author: M.M. Alipour (Assistant Professor)
E-mail address: m.mollaalipour@umz.ac.ir
http://dx.doi.org/10.22084/jrstan.2019.18781.1090
ISSN: 2588-2597

T	Elevated temperature	v	Poisson's ratio
U	Potential energy	W	Work of the applied loads
k_w	Winkler's coefficient	k_s	Pasternak's coefficient
Y_N	Space of test functions	β	Number of boundary conditions
$s(z)$	Porous distribution in thickness direction		

1. Introduction

Sandwich structures are widely applied in various fields. These structures may be designed based on the specified purposes, for example may be fabricated by heterogeneous materials, subjected to non-uniform load and hygrothermal environment, resting on elastic foundation, etc. Thus, the analysis of these structures and the development of a new approach are very important. The analysis of one-directional functionally graded beam with variation of the material properties in thickness [1, 2] or axial direction [3, 4] have been extensively studied by many researchers. However, the studies on bi-dimensional functionally graded (BDFG) beam are very far and few between, even for single layer beams. Based on the exponential variation of Young's modulus in the thickness and axial directions, Lu et al. [5] analyzed the bending of bi-direction FG beams. The dynamic response of BDFG beams were investigated by Deng and Cheng [6]. Wang et al. [7] analyzed the free vibration analysis of BDFG beam in which the material properties vary based on a power law gradation in thickness direction and exponentially in axial direction. Free vibration, buckling and dynamic analyses of BDFG microbeam embedded in elastic foundation were investigated by Chen et al. [8]. Chen et al. [9] investigated the static and dynamic responses of BDFG microbeams based on the third-order shear deformation beam theory. Simsek studied the buckling [10] and dynamic response of BDFG beams under moving load [11]. Li et al. [12] examined bending behavior of BDFG beam structures based on a proposed meshless Total Lagrangian (TL) Corrective Smoothed Particle Method (CSPM). General non-uniform material-varying micro-beam models under a moving harmonic load/mass were investigated by Rajasekaran and Khaniki [13]. Nguyen and Lee [14] analyzed the static behaviors of thin-walled BDFG beams. Free vibration of BDFG circular beams was investigated by Fariborz and Batra [15] based on shear deformation theory. Karamanli [16] analyzed the free vibration of BDFG beams. Pydah and Sabale [17] conducted a static analysis of BDFG curved beams based on the Euler-Bernoulli theory. Postbuckling analysis of BDFG imperfect beams was investigated by Lei et al. [18]. Bending and stress [19] and free vibration [20] analyses of circular plates with variation of the material properties in the radial and thickness directions, were performed by Alipour and Shariyat. Spectral methods have been used extensively for various applications in the last two decades because of their good rate of convergence for sufficiently smooth functions [21]. Shariyat et al. [22] investigated material heterogeneity on stress and free vibration of the circular plates. Chebyshev tau method is a particularly efficient spectral approach in which Chebyshev polynomials are used in the tau method of Lanczos [23]. Numerical programs using this technique are often considerably faster with greater accuracy than other standard methods such as finite differencing [24]. Etehadi and Botshekanan Dehkordi [25] investigated the functionally graded sandwich beam and analyzed the effect of axial stresses of the core. Based on three-dimensional theory of elasticity, Shaban [26] carried out a static analysis of sandwich structures with sinusoidal corrugated cores. Recently there have been several published papers on the applications of the tau method. Siyyam and Syam [27] presented the CTM for the two-dimensional Poisson equation. Ahmadi and Adibi [28] applied the Chebyshev tau method for the Laplace equation. Saadatmandi and Dehghan [29] utilized the CTM to approximate the solution of hyperbolic telegraph problem. Wang [30] applied a time-splitting Chebyshev tau spectral method to the Ginzburg-Landau-Schrödinger equation with zero/nonzero far-field boundary conditions. Saravi [31] proposed the CTM for solving linear ordinary differential equations. The presented study examined the bending and stress analysis of BDFG porous sandwich beams under non-uniform load resting on Winkler/Pasternak foundation in hygrothermal environment. In the most of the previous publications, analysis was conducted using the equivalent single layer theories, and therefore they are limited to the analysis of single layer beams. In this study, to overcome the shortcomings of the single layer theories in the analysis of multilayer structures [32, 33], governing equations are obtained based on the layerwise theory [34–37]. The chebyshev tau spectral scheme is employed to solve the five coupled differential equations. The effectiveness of the proposed solution procedure is demonstrated by the comparison of the obtained results with those extracted from the ABAQUS software. In section 2, a three-layer sandwich beam is investigated. Next, the CTM is described briefly in section 3. The fourth section is devoted to applying the CTM and obtaining the results. In section 5, some examples are given to show the accuracy, validity and applicability of the technique. Finally, the conclusions are presented in section 6.

2. Governing Equations of the FG Three-layered Sandwich Beams

As shown in Fig. 1, a three-layer sandwich beam with regard to non-uniform normal load is investigated. The thickness of the top and bottom face sheets and core are denoted respectively by h_t, h_b and h_c.

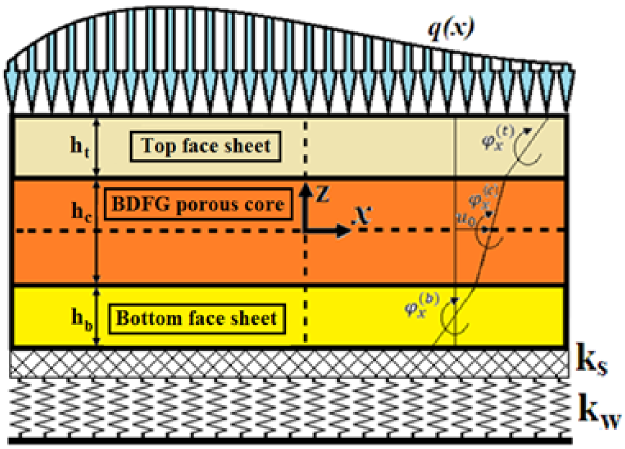

Fig. 1. Schematic of the BDFG porous sandwich beam resting on Winkler/Pasternak foundation.

For sandwich beams with two directionally functionally graded porous cores, the elastic moduli can be expressed as:

$$\begin{aligned} E_c(x,z) &= \bar{E}_c[1-s(z)f(x)], \\ G_c(x,z) &= \frac{E_c(x,z)}{2(1+v_c)'} \end{aligned} \tag{1}$$

where $s(z)$ and $f(x)$ are the porous distribution in thickness and longitudinal directions. Two patterns are examined for the porous distribution in thickness direction.

Pattern A (uniform porosity distribution): $s(z) = s_0$

Pattern B (non-uniform porosity distribution): (2)

$$s(z) = s_0 \cos\left[\left(\frac{\pi}{2}\right)\frac{z}{h_c} + \left(\frac{\pi}{4}\right)\right]$$

Based on the theory of layerwise, the displacement field of the layers can be expressed as:

$$\begin{cases} u_t = u_0 + \left(z - \dfrac{h_c}{2}\right)\varphi_x^{(t)} + \dfrac{h_c}{2}\varphi_x^{(c)}, \\ \qquad \dfrac{h_c}{2} \le z \le \dfrac{h_c}{2} + h_t, \\ u_c = u_0 + z\varphi_x^{(c)}, \qquad -\dfrac{h_c}{2} \le z \le \dfrac{h_c}{2}, \\ u_b = u_0 + \left(z + \dfrac{h_c}{2}\right)\varphi_x^{(b)} - \dfrac{h_c}{2}\varphi_x^{(c)}, \\ \qquad -h_b - \dfrac{h_c}{2} \le z \le -\dfrac{h_c}{2}, \\ w = w_0(x) \end{cases} \tag{3}$$

where u_t, u_c and u_b are the in-plane displacement of the top, core and bottom layers, $\varphi_x^{(t)}$, $\varphi_x^{(c)}$ and $\varphi_x^{(b)}$ are the rotation of the top, core and bottom layers and w is the transverse displacement of sandwich beam. For small deflections of beam, strains of each layer are given as:

$$\varepsilon_x^{(i)} = \frac{\partial u_i}{\partial x}, \quad \gamma_{xz}^{(i)} = \frac{\partial u_i}{\partial z} + \frac{\partial w_i}{\partial x}, \qquad i = t, c, b \tag{4}$$

The present heterogeneous porous beam is subjected to moisture exposure C and elevated temperature T.

$$\begin{aligned} \sigma_x^{(i)} &= \frac{E_i}{1-v_i^2}\varepsilon_x^{(i)} - \frac{E_i}{1-v_i}(\alpha^{(i)}\Delta T + \beta^{(i)}\Delta C) \\ \tau_{xz}^{(i)} &= \frac{E_i}{2(1+v_i)}\gamma_{xz}^{(i)}, \qquad i = t, c, b \end{aligned} \tag{5}$$

E is Young's modulus, v is Poisson's ratio, $\alpha^{(i)}$ and $\beta^{(i)}$ are the thermal expansion and moisture concentration coefficients. The principle of minimum total potential energy is used for derivation of the governing equations as:

$$\delta II = \delta U - \delta W = 0 \tag{6}$$

where U is the potential energy and W is the work of the applied loads:

$$\begin{aligned} \delta U &= \int_l \int_{\frac{h_c}{2}}^{\frac{h_c}{2}+h_t} \left(\sigma_x^{(t)}\delta\varepsilon_x^{(t)} + \tau_{xz}^{(t)}\delta\gamma_{xz}^{(t)}\right) dzdx \\ &+ \int_l \int_{-\frac{h_c}{2}}^{\frac{h_c}{2}} \left(\sigma_x^{(c)}\delta\varepsilon_x^{(c)} + \tau_{xz}^{(c)}\delta\gamma_{xz}^{(c)}\right) dzdx \\ &+ \int_l \int_{-\frac{h_c}{2}-h_b}^{-\frac{h_c}{2}} \left(\sigma_x^{(b)}\delta\varepsilon_x^{(b)} + \tau_{xz}^{(b)}\delta\gamma_{xz}^{(b)}\right) dzdx \end{aligned} \tag{7}$$

$$\delta W = \int_l (q(x) + k_w - k_s w_{,xx})\delta w dx \tag{8}$$

k_w and k_s are Winkler's and Pasternak's coefficients of the elastic foundation, respectively.

Based on Eqs. (3) to (8), the governing equations of the beam are:

$$\begin{aligned} &\delta u_0 \ne 0 : N_{x,x}^{(t)} + N_{x,x}^{(c)} + N_{x,x}^{(b)} = 0, \\ &\delta\varphi_x^{(t)} \ne 0 : M_{x,x}^{(t)} - \frac{h_c}{2}N_{x,x}^{(t)} - Q_x^{(t)} = 0, \\ &\delta\varphi_x^{(c)} \ne 0 : M_{x,x}^{(c)} + \frac{h_c}{2}\left(N_{x,x}^{(t)} - N_{x,x}^{(b)}\right) - Q_x^{(c)} = 0, \\ &\delta\varphi_x^{(b)} \ne 0 : M_{x,x}^{(b)} + \frac{h_c}{2}N_{x,x}^{(b)} - Q_x^{(b)} = 0, \\ &\delta w \ne 0 : Q_{x,x}^{(t)} + Q_{x,x}^{(c)} + Q_{x,x}^{(b)} - k_w w + k_s w_{,xx} = q(x), \end{aligned} \tag{9}$$

where

$$\begin{cases} N_x^{(t)} = A^{(t)}u_{0,x} + \left(B^{(t)} - \dfrac{h_c}{2}A^{(t)}\right)\varphi_{x,x}^{(t)} + \dfrac{h_c}{2}A^{(t)}\varphi_{x,x}^{(c)} - (1+v_t)A^{(t)}\left(\alpha^{(t)}\Delta T + \beta^{(t)}\Delta C\right), \\ M_x^{(t)} = B^{(t)}u_{0,x} + \left(D^{(t)} - \dfrac{h_c}{2}B^{(t)}\right)\varphi_{x,x}^{(t)} + \dfrac{h_c}{2}B^{(t)}\varphi_{x,x}^{(c)} - (1+v_t)B^{(t)}\left(\alpha^{(t)}\Delta T + \beta^{(t)}\Delta C\right), \end{cases} \tag{10}$$

$$\begin{cases} N_x^{(c)} = A^{(c)}u_{0,x} + B^{(c)}\varphi_{x,x}^{(c)} - (1+v_c)A^{(c)}\left(\alpha^{(c)}\Delta T + \beta^{(c)}\Delta C\right), \\ M_x^{(c)} = B^{(c)}u_{0,x} + D^{(c)}\varphi_{x,x}^{(c)} - (1+v_c)B^{(c)}\left(\alpha^{(c)}\Delta T + \beta^{(c)}\Delta C\right), \end{cases} \tag{11}$$

$$\begin{cases} N_x^{(b)} = A^{(b)}u_{0,x} + \left(B^{(b)} + \dfrac{h_c}{2}A^{(b)}\right)\varphi_{x,x}^{(b)} - \dfrac{h_c}{2}A^{(b)}\varphi_{x,x}^{(c)} - (1+v_b)A^{(b)}\left(\alpha^{(b)}\Delta T + \beta^{(b)}\Delta C\right), \\ M_x^{(b)} = B^{(b)}u_{0,x} + \left(D^{(b)} + \dfrac{h_c}{2}B^{(b)}\right)\varphi_{x,x}^{(b)} - \dfrac{h_c}{2}B^{(b)}\varphi_{x,x}^{(c)} - (1+v_b)B^{(b)}\left(\alpha^{(b)}\Delta T + \beta^{(b)}\Delta C\right), \end{cases} \tag{12}$$

$$\begin{aligned} Q_x^{(t)} &= \bar{A}^{(t)}\left(\varphi_x^{(t)} + w_{,x}\right), \\ Q_x^{(c)} &= \bar{A}^{(c)}\left(\varphi_x^{(c)} + w_{,x}\right), \\ Q_x^{(b)} &= \bar{A}^{(b)}\left(\varphi_x^{(b)} + w_{,x}\right), \end{aligned} \tag{13}$$

$x \in l = [-1, 1]$ and $q(x)$ is the arbitrary distributed transverse load of the top surface of the sandwich beam. $A^{(i)}$, $B^{(i)}$, $D^{(i)}$ and $\bar{A}^{(i)}$ for $i = t, c, b$ are defined as:

$$\begin{aligned} \begin{Bmatrix} A^{(t)} \\ B^{(t)} \\ D^{(t)} \end{Bmatrix} &= \int_{\frac{h_c}{2}}^{\frac{h_c}{2}+h_t} \frac{E_t}{1-v_t^2}\begin{Bmatrix} 1 \\ z \\ z^2 \end{Bmatrix} dz, \\ \begin{Bmatrix} A^{(c)} \\ B^{(c)} \\ D^{(c)} \end{Bmatrix} &= \int_{-\frac{h_c}{2}}^{\frac{h_c}{2}} \frac{E_c}{1-v_c^2}\begin{Bmatrix} 1 \\ z \\ z^2 \end{Bmatrix} dz, \\ \begin{Bmatrix} A^{(b)} \\ B^{(b)} \\ D^{(b)} \end{Bmatrix} &= \int_{-\frac{h_c}{2}-h_b}^{-\frac{h_c}{2}} \frac{E_b}{1-v_b^2}\begin{Bmatrix} 1 \\ z \\ z^2 \end{Bmatrix} dz, \end{aligned} \tag{14}$$

$$\begin{aligned} \bar{A}^{(t)} &= \int_{\frac{h_c}{2}}^{\frac{h_c}{2}+h_t} \frac{E_t}{2(1+v_t)}dz, \\ \bar{A}^{(c)} &= \int_{-\frac{h_c}{2}}^{\frac{h_c}{2}} \frac{E_c}{2(1+v_c)}dz, \\ \bar{A}^{(b)} &= \int_{-\frac{h_c}{2}-h_b}^{-\frac{h_c}{2}} \frac{E_b}{2(1+v_b)}dz \end{aligned} \tag{15}$$

The governing equations of the FG three-layered sandwich beam can be expressed as:

$$\begin{aligned} &\left(A^{(t)} + A^{(c)} + A^{(b)}\right)u_{0,xx} + \left(B^{(t)} - \frac{h_c}{2}A^{(t)}\right)\varphi_{x,xx}^{(t)} \\ &+ \left(\frac{h_c}{2}A^{(t)} + B^{(c)} - \frac{h_c}{2}A^{(b)}\right)\varphi_{x,xx}^{(c)} \\ &+ \left(B^{(b)} + \frac{h_c}{2}A^{(b)}\right)\varphi_{x,xx}^{(b)} + A_{,x}^{(c)}u_{0,x} + B_{,x}^{(c)}\varphi_{x,x}^{(c)} \\ &- (1+v_c)A_{,x}^{(c)}(\alpha^{(c)}\Delta T + \beta^{(c)}\Delta C) = 0 \end{aligned} \tag{16}$$

$$\begin{aligned} &\left(B^{(t)} - \frac{h_c}{2}A^{(t)}\right)u_{0,xx} + \left(D^{(t)} - h_cB^{(t)} + \frac{h_c^2}{4}A^{(t)}\right)\varphi_{x,xx}^{(t)} \\ &+ \left(\frac{h_c}{2}B^{(t)} - \frac{h_c^2}{4}A^{(t)}\right)\varphi_{x,xx}^{(c)} \\ &- \bar{A}^{(t)}\left(\varphi_x^{(t)} + w_{,x}\right) = 0, \end{aligned} \tag{17}$$

$$\begin{aligned} &\left(\frac{h_c}{2}A^{(t)} + B^{(c)} - \frac{h_c}{2}A^{(b)}\right)u_{0,xx} \\ &+ \left(\frac{h_c}{2}B^{(t)} - \frac{h_c^2}{4}A^{(t)}\right)\varphi_{x,xx}^{(t)} \\ &+ \left(\frac{h_c^2}{4}A^{(t)} + D^{(c)} + \frac{h_c^2}{4}A^{(b)}\right)\varphi_{x,xx}^{(c)} \\ &- \left(\frac{h_c}{2}B^{(b)} + \frac{h_c^2}{4}A^{(b)}\right)\varphi_{x,xx}^{(b)} - \bar{A}^{(c)}\left(\varphi_x^{(c)} + w_{,x}\right) \\ &+ B_{,x}^{(c)}u_{0,x} + D_{,x}^{(c)}\varphi_{x,x}^{(c)} \\ &- (1+v_c)B_{,x}^{(c)}(\alpha^{(c)}\Delta T + \beta^{(c)}\Delta C) = 0, \end{aligned} \tag{18}$$

$$\begin{aligned} &\left(B^{(b)} + \frac{h_c}{2}A^{(b)}\right)u_{0,xx} - \left(\frac{h_c}{2}B^{(b)} + \frac{h_c^2}{4}A^{(b)}\right)\varphi_{x,xx}^{(c)} \\ &+ \left(\frac{h_c^2}{4}A^{(b)} + h_cB^{(b)} + D^{(b)}\right)\varphi_{x,xx}^{(b)} \\ &- \bar{A}^{(b)}\left(\varphi_x^{(b)} + w_{,x}\right) = 0, \end{aligned} \tag{19}$$

$$\begin{aligned} &\bar{A}^{(t)}\varphi_{x,x}^{(t)} + \bar{A}^{(c)}\varphi_{x,x}^{(c)} + \bar{A}^{(b)}\varphi_{x,x}^{(b)} \\ &+ \left(\bar{A}^{(t)} + \bar{A}^{(c)} + \bar{A}^{(b)}\right)w_{,xx} \\ &+ \bar{A}_{,x}^{(c)}\left(\varphi_x^{(c)} + w_{,x}\right) - k_w w + k_s w_{,xx} = q(x). \end{aligned} \tag{20}$$

The general edge conditions can be written as:

$$\begin{cases} u_0 = 0 \quad \text{or} \quad N_x^{(t)} + N_x^{(c)} + N_x^{(b)} = 0, \\ \varphi_x^{(t)} = 0 \quad \text{or} \quad M_x^{(t)} - \dfrac{h_c}{2}N_x^{(t)} = 0, \\ \varphi_x^{(c)} = 0 \quad \text{or} \quad \dfrac{h_c}{2}N_x^{(t)} + M_x^{(c)} - \dfrac{h_c}{2}N_x^{(b)} = 0, \\ \varphi_x^{(b)} = 0 \quad \text{or} \quad M_x^{(b)} + \dfrac{h_c}{2}N_x^{(b)} = 0, \\ w = 0 \quad \text{or} \quad Q_x^{(t)} + Q_x^{(c)} + Q_x^{(b)} = 0. \end{cases} \tag{21}$$

The Clamped-Clamped (C-C) boundary condition can be derived as:

$$u_0(\pm 1) = \varphi_x^{(t)}(\pm 1) = \varphi_x^{(c)}(\pm 1) \\ = \varphi_x^{(b)}(\pm 1) = w(\pm 1) = 0 \tag{22}$$

3. The Tau Method

Some fundamental results for Chebyshev approximation [38] are needed. The Chebyshev polynomial of degree n on $[-1, 1]$ is defined by the formula as:

$$T_n(\cos\theta) = \cos n\theta \tag{23}$$

For $x \in [-1, 1]$, we have the following recurrence relation:

$$\begin{aligned} &T_{n+1}(x) = 2xT_n(x) - T_{n-1}(x), \qquad n > 0 \\ &T_0(x) = 1 \\ &T_1(x) = x \end{aligned} \tag{24}$$

They form an orthonormal basis with respect to the weighted scalar product:

$$\begin{aligned} &(u, v)_\omega = \left(\int_{-1}^{1} u(x)v(x)\omega(x)dx \right), \\ &\omega(x) = \frac{1}{\sqrt{1-x^2}}, \qquad x \in [-1, 1] \end{aligned} \tag{25}$$

Proposition 1: The polynomials $T_n(x)$ are orthogonal, i.e.,

$$(T_n(x), T_m(x))_\omega = \frac{\pi}{2} c_n \delta_{n,m}, \quad m, n \in \mathbb{N} \tag{26}$$

where

$$\delta_{n,m} = \begin{cases} 0, & n \neq m, \\ 1, & n = m, \end{cases} \tag{27}$$

and the coefficients c_n are:

$$c_n = \begin{cases} 2, & n = 0, \\ 1, & n > 0. \end{cases} \tag{28}$$

Some useful properties of Chebyshev polynomials are [39]:

$$\begin{aligned} &|T_n(x)| \le 1, & &|x| \le 1, \\ &T_n(-x) = (-1)^n T_n(x), & &T_n(\pm 1) = (\pm 1)^n, \end{aligned} \tag{29}$$

$$T_n(x)T_m(x) = \frac{T_{n+m}(x) + T_{|n-m|}(x)}{2} \tag{30}$$

The Chebyshev expansion of a function $u(x)$ is:

$$u(x) = \sum_{n=0}^{\infty} b_n T_n(x), \quad b_n = \frac{2}{\pi c_n}(u, T_n(x))_\omega \tag{31}$$

Consider the expansion of a function $u(x)$ or its derivatives in terms of Chebyshev polynomials on the interval $[-1, 1]$. Suppose that u and its derivatives can be expanded as:

$$u(x) = \sum_{n=0}^{\infty} b_n^{(0)} T_n(x), \quad \frac{d^m u}{dx^m} = \sum_{n=0}^{\infty} b_n^{(m)} T_n(x), \\ m = 0, 1, \ldots \tag{32}$$

Then recursion relation below is obtained:

$$c_{n-1} b_{n-1}^{(m)} = 2n b_n^{(m-1)} + b_{n+1}^{(m)}, \quad n \ge 1 \tag{33}$$

gives:

$$\begin{aligned} &c_n b_n^{(1)} = 2 \sum_{\substack{p=n+1 \\ p+n \text{ odd}}}^{\infty} p b_n, \\ &c_n b_n^{(2)} = 2 \sum_{\substack{p=n+2 \\ p+n \text{ even}}}^{\infty} p[p^2 - n^2] b_p, \quad n \ge 0, \end{aligned} \tag{34}$$

where c_n is defined by (28). The formulae given above are used to expand products of Chebyshev polynomials and derivatives of Chebyshev polynomials as expansions in Chebyshev polynomials. For instance, if a function $u(x)$ and its first and second derivatives $u'(x)$ and $u''(x)$ have series expansions in terms of Chebyshev polynomials, then we have:

$$\begin{aligned} u(x) &= \sum_{n=0}^{N} b_n T_n(x), \\ u'(x) &= \sum_{n=0}^{N-1} b_n^{(1)} T_n(x), \\ u''(x) &= \sum_{n=0}^{N-2} b_n^{(2)} T_n(x), \end{aligned} \tag{35}$$

then the coefficients $b_n^{(1)}$ and $b_n^{(2)}$ are related to the coefficients b_n, by:

$$\begin{aligned} &c_n b_n^{(1)} = 2 \sum_{\substack{p=n+1 \\ p+n \text{ odd}}}^{p=N} p b_p, \\ &c_n b_n^{(2)} = 2 \sum_{\substack{p=n+2 \\ p+n \text{ even}}}^{p=N} p[p^2 - n^2] b_p, \end{aligned} \tag{36}$$

where c_n is defined by (28). The tau approach was first suggested by Lanczos [23] and its use with Chebyshev polynomials was later widely developed by Fox [40] and was applied by Orszag to an extensive variety of problems [41]. Consider the following linear boundary value problem:

$$(LP) \begin{cases} \mathcal{L}u = f, & x \in (-1, 1), \\ Bu = 0, \end{cases} \tag{37}$$

where $\mathcal{L}$ is a linear differential operator acting in a Hilbert space, X and B stands for a set of linear differential operators defined on -1 and 1. A Hilbert space [42] is a vector space equipped with a scalar product for which all the Cauchy sequences are convergent. The scalar product structure of a Hilbert space helps us to introduce the concept of orthogonality. An orthogonal basis of a Hilbert space is an orthogonal set such that every vector in the space can be expanded in terms of the basis. The Chebyshev tau method is characterized by the following choice:

$$\begin{aligned} &X = \mathcal{L}^2_\omega(-1,1), \quad X_N = \{v \in \mathcal{P}_N | Bv = 0\}, \\ &Y_N = \mathcal{P}_{N-\beta}, \end{aligned} \tag{38}$$

Where $\mathcal{L}^2_\omega(-1,1)$ is the space of functions v so that the norm

$$||v||_\omega = \left(\int_{-1}^{1} |v(x)|^2 \omega(x) dx \right)^{\frac{1}{2}} \tag{39}$$

is finite [43], X_N denotes the space of trial or shape functions and Y_N is that of test functions. Moreover, $\mathcal{P}_N$ is the space of algebraic polynomials of degree at most $N \in \mathbb{N}$, $N > 0$ and β stands for the number of boundary conditions. Accepting the family $\{T_n,\ n = 0, 1, 2, \ldots, N\}$ as a basis for the finite dimensional space X_N and the family $\{T_m,\ m = 0, 1, 2, \ldots, N-\beta\}$ as a set of "test" functions in Y_N, the variational formulation corresponding to (37) is:

$$\begin{cases} \text{find the coefficients } b_n \text{ of } u_N(x) \in \mathcal{P}_N, \\ u_N(x) = \displaystyle\sum_{n=0}^{N} b_n T_n(x), \qquad \text{such that} \\ \displaystyle\int_{-1}^{1} (\mathcal{L}u_N(x) - f(x)) \psi_m dx = 0, \\ \qquad\qquad m = 0, 1, 2, \ldots, N-\beta, \\ \displaystyle\sum_{n=0}^{N} b_n B(T_n) = 0 \end{cases} \tag{40}$$

where ψ_m is:

$$\psi_m(x) = \frac{2}{\pi c_m} T_m(x) \omega(x) = \frac{2}{\pi c_m} T_m(x) \frac{1}{\sqrt{1-x^2}} \tag{41}$$

4. Application of Chebyshev Tau Method

In order to solve the differential equation system (16)-(20) regarding boundary condition (22) by CTM, we expand the solution functions u_0, w and $\varphi_x^{(i)}$, ($i = t, c, b$) as a finite series of basis functions $\{T_n(x)\}_{n=0}^N$ as given below:

$$\begin{aligned} (u_0)_N(x) &= \sum_{n=0}^{N} b_n T_n(x), \\ w_N(x) &= \sum_{n=0}^{N} a_n T_n(x), \\ (\varphi_x^{(i)})_N(x) &= \sum_{n=0}^{N} cj_n T_n(x), \quad i = t, c, b, \quad j = 1, 2, 3\cdot \end{aligned} \tag{42}$$

We will need the first and second order derivatives of $(u_0)_N(x)$, $(\varphi_x^{(i)})_N(x)$, $i = t, c, b$ and $w_N(x)$ as they relate to $T_n(x)$. To this end, equations (36) will be used.

$$\frac{d(u_0)_N}{dx} = \sum_{n=0}^{N-1} b_n^{(1)} T_n(x), \quad \frac{d^2(u_0)_N}{dx^2} = \sum_{n=0}^{N-2} b_n^{(2)} T_n(x), \tag{43}$$

$$\begin{aligned} \frac{d(\varphi_x^{(i)})_N}{dx} &= \sum_{n=0}^{N-1} cj_n^{(1)} T_n(x), \\ \frac{d^2(\varphi_x^{(i)})_N}{dx^2} &= \sum_{n=0}^{N-2} cj_n^{(2)} T_n(x), \quad i = t, c, b, \ j = 1, 2, 3, \end{aligned} \tag{44}$$

$$\frac{dw_N}{dx} = \sum_{n=0}^{N-1} a_n^{(1)} T_n(x), \quad \frac{d^2 w_N}{dx^2} = \sum_{n=0}^{N-2} a_n^{(2)} T_n(x)\cdot \tag{45}$$

we put

$$\begin{aligned} &A = \sum_{n=0}^{N} A_n T_n(x), \quad B = \sum_{n=0}^{N} B_n T_n(x), \\ &D = \sum_{n=0}^{N} D_n T_n(x), \\ &\bar{A} = \sum_{n=0}^{N} \bar{A}_n T_n(x), \quad q(x) = \sum_{n=0}^{N} q_n T_n(x), \end{aligned} \tag{46}$$

where

$$\begin{aligned} A_n &= \frac{2}{\pi c_n}(A, T_n(x))_w, \quad B_n = \frac{2}{\pi c_n}(B, T_n(x))_w, \\ D_n &= \frac{2}{\pi c_n}(D, T_n(x))_w, \\ \bar{A}_n &= \frac{2}{\pi c_n}(\bar{A}, T_n(x))_w, \quad q_n = \frac{2}{\pi c_n}(q(x), T_n(x))_w. \end{aligned} \tag{47}$$

The substitution of Eqs. (42) and (46) into the system (16)-(20) yields an algebraic equation system. The first step will be to take the inner product of the obtained equation system with $\psi_m(x)$ where

$$\begin{aligned} (T_n(x), \psi_m(x)) &= \frac{2}{\pi c_m} \int_{-1}^{1} T_n(x) T_m(x) \frac{1}{\sqrt{1-x^2}} dx \\ &= \delta_{n,m}, \quad m = 0, 1, \ldots, N-2. \end{aligned} \tag{48}$$

Let

$$\begin{aligned} &N = 3, \qquad q(x) = 1 - 2x + x^2, \quad h_t = h_b = 0.1 \\ &h_c = 0.2, \quad v_t = v_c = v_b = 0.3, \end{aligned}$$

$$E_t = 2, \qquad E_c = 1 + 0.6x - 0.2x^2, \qquad E_b = 3$$
$$k_w = k_s = 0, \quad (\alpha^{(i)}\Delta T + \beta^{(i)}\Delta C) = 0, \quad i = t, c, b.$$

Using the recurrence relationships for the first and second derivative expansion coefficients from (36) and orthogonality properties of the Chebyshev polynomials, the resulted algebraic equation system leads to:

$$\begin{aligned}
&(2.81319)b_2 + (1.97802)b_3 + (4.39560\times10^{-2})c1_2\\
&\quad - (4.39560\times10^{-2})c2_2 - (6.59340\times10^{-2})c3_2\\
&\quad + (1.31868\times10^{-1})b_1 = 0,\\
&(1.71428\times10)b_3 + (1.05494)b_2\\
&\quad + (2.63736\times10^{-1})c1_3 - (2.63736\times10^{-1})c2_3\\
&\quad - (3.95604\times10^{-1})c3_3 - (8.79120\times10^{-2})b_1\\
&\quad = 0,\\
&(4.39560\times10^{-2})b_2 + (2.93040\times10^{-3})c1_2\\
&\quad + (4.39560\times10^{-3})c2_2 - (7.69231\times10^{-2})c1_0\\
&\quad - (7.69231\times10^{-2})a_1 - (2.30769\times10^{-1})a_3 = 0,\\
&(2.63736\times10^{-1})b_3 + (1.75824\times10^{-2})c1_3\\
&\quad + (2.63736\times10^{-2})c2_3 - (7.69231\times10^{-2})c1_1\\
&\quad - (3.07692\times10^{-1})a_2 = 0,\\
&-(6.92307\times10^{-2})a_1 - (9.23075\times10^{-2})a_2\\
&\quad - (1.84615\times10^{-1})a_3 + (2.78755\times10^{-2})c2_2\\
&\quad - (2.26373\times10^{-2})c2_1 + (6.59338\times10^{-3})c2_3\\
&\quad - (6.92307\times10^{-2})c2_0 - (4.39560\times10^{-2})b_2\\
&\quad + (4.39560\times10^{-3})c1_2 + (6.59340\times10^{-3})c3_2 = 0,\\
&-(2.61538\times10^{-1})a_2 - (1.95604\times10^{-2})c2_2\\
&\quad - (2.76923\times10^{-1})a_3 - (4.61538\times10^{-2})a_1\\
&\quad + (1.48901\times10^{-1})c2_3 - (6.56776\times10^{-2})c2_1\\
&\quad - (4.61538\times10^{-2})c2_0 - (2.63736\times10^{-1})b_3\\
&\quad - (2.63736\times10^{-2})c1_3 - (3.95604\times10^{-2})c3_3 = 0,\\
&-(6.59340\times10^{-2})b_2 + (6.59340\times10^{-3})c2_2\\
&\quad + (4.39560\times10^{-3})c3_2 - (1.15385\times10^{-1})c3_0\\
&\quad - (1.15385\times10^{-1})a_1 - (3.46155\times10^{-1})a_3 = 0,\\
&-(3.95604\times10^{-1})b_3 + (3.95604\times10^{-2})c2_3\\
&\quad + (2.63736\times10^{-2})c3_3 - (1.15385\times10^{-1})c3_1\\
&\quad - (4.61540\times10^{-1})a_2 = 0,\\
&-(1.50000) + (6.92306\times10^{-1})a_3\\
&\quad + (1.15385\times10^{-1})c3_1 + (3.46155\times10^{-1})c3_3\\
&\quad + (1.84615\times10^{-1})c2_3 + (7.69231\times10^{-2})c1_1\\
&\quad + (2.30769\times10^{-1})c1_3 + (4.61538\times10^{-2})a_1\\
&\quad + (9.84612\times10^{-1})a_2 + (9.23075\times10^{-2})c2_2\\
&\quad + (5.38461\times10^{-2})c2_1 + (4.61538\times10^{-2})c2_0 = 0,\\
&2 + (4.61540\times10^{-1})c3_2 + (3.07692\times10^{-1})c1_2\\
&\quad + (3.69230\times10^{-1})a_2 + (2.46154\times10^{-1})c2_2\\
&\quad + 6a_3 - (3.07692\times10^{-2})a_1 + (2.76923\times10^{-1})c2_3\\
&\quad + (9.23076\times10^{-2})c2_1 - (3.07692\times10^{-2})c2_0 = 0
\end{aligned} \tag{49}$$

Using the Chebyshev expansions of (42), the boundary condition (22) can be written as:

$$\begin{cases}
b_0 - b_1 + b_2 - b_3 = 0,\\
b_0 + b_1 + b_2 + b_3 = 0,\\
a_0 - a_1 + a_2 - a_3 = 0,\\
a_0 + a_1 + a_2 + a_3 = 0,\\
cj_0 - cj_1 + cj_2 - cj_3 = 0,\\
cj_0 + cj_1 + cj_2 + cj_3 = 0, \quad j = 1, 2, 3.
\end{cases} \tag{50}$$

The solutions to (49) plus the ten boundary equations (50) are

$$\begin{cases}
a = 10^{-1}(-7.51587, 3.12334, 7.51587, -3.12334),\\
b = 10^{-2}(9.55881\times10^{-1}, -1.82028,\\
\qquad -9.55881\times10^{-1}, 1.82028),\\
c_1 = (6.22902\times10^{-1}, -2.46093,\\
\qquad -6.22902\times10^{-1}, 2.46093),\\
c_2 = 10^{-1}(-4.79992, 2.31853, 4.79992,\\
\qquad -2.31853),\\
c_3 = (6.33427\times10^{-1}, -2.56253,\\
\qquad -6.33427\times10^{-1}, 2.56253).
\end{cases} \tag{51}$$

The substitution of (51) into the (42) leads to

$$\begin{cases}
(u_0)_3(x) = 10^{-2}((1.91176) - (7.28112)x\\
\qquad - (1.91176)x^2 + (7.28112)x^3),\\
(\varphi_x^{(t)})_3(x) = (1.24580) - (9.84372)x - (1.24580)x^2\\
\qquad + (9.8437)x^3,\\
(\varphi_x^{(c)})_3(x) = 10^{-1}((-9.59984) + (9.27412)x\\
\qquad + (9.59984)x^2 - (9.27412)x^3),\\
(\varphi_x^{(b)})_3(x) = (1.26685) - (1.02501\times10)x\\
\qquad - (1.26685)x^2 + (1.02501\times10)x^3,\\
w_3(x) = (-1.50317) + (1.2493)x + (1.50317)x^2\\
\qquad - (1.24934)x^3.
\end{cases} \tag{52}$$

5. Results and Comparisons

In this section, different examples of bi-directional functionally graded (BDFG) porous sandwich beams are investigated. To demonstrate the accuracy and reliability of the Chebyshev tau approach, the obtained results of BDFG porous sandwich beam are compared with the extracted results of ABAQUS software using the finite element method. The following dimensionless quantities are applied for presented results in which the elastic moduli of the face sheets and external load are normalized based on the elastic modulus of the core.

$$\begin{aligned}
\bar{u}_0 &= \frac{u_0}{h_c}\times10^6, & \bar{w} &= \frac{w}{h_c}\times10^6,\\
\bar{s}_x &= \frac{s_x}{P}, & \bar{q} &= \frac{q}{\bar{E}_c}\times10^6,\\
\bar{k}_w &= \frac{k_w h_c}{\bar{E}_c}, & \bar{k}_s &= \frac{k_s}{L\bar{E}_c}.
\end{aligned} \tag{53}$$

In all examples, it is assumed that $q = (1 - 2x + x^2)\bar{E}_c$, $E_t = 2\bar{E}_c$, $E_b = 3\bar{E}_c$, $v_t = v_c = v_b = 0.3$, $h_t = h_b = 0.1$, $h_c = 0.2$ and $L = 2$. Moreover, $k_w = k_s$ and $\Delta T = \Delta C = 0$ unless stated otherwise.

Example 1. In this example, the results of FG three-layerd sandwich beams subjected to nun-uniform load are obtained. Obtained results of sandwich beam with FG core are presented and a comparison with the extracted results of ABAQUS software are performed. The variation of the material properties of core in the axial direction is assumed as $E_c = (1+0.6x-0.2x^2)\bar{E}_c$ in which Young's modulus of core vary from $E_c = 0.2\bar{E}_c$ to $E_c = 1.4\bar{E}_c$ as parabolic function. In the finite element simulation of functionally graded beam using the ABAQUS software, variations of the material properties are modeled by dividing each layer into a sufficient number of sections (e.g., 40 sections) to estimate the gradual variations of the material properties. Also, the width of the considered beam in the ABAQUS software is 0.1. First of all, a sensitivity analysis of the number of terms of the finite series solution had to be conducted to achieve reliable and sufficiently accurate results. Table 1 shows the values of transverse deflection of clamped-clamped sandwich beam for different amounts of terms of the finite series (N).

It can be seen that increasing the number of polynomial items improves the accuracy of the results and leads to convergent solutions at $N = 15$. It is observed that choosing 15 terms of the finite series solution may lead to a convergent solution.

However, 20 terms of the finite series solution are used for solving the governing differential equations to ensure that the convergence may not be altered by various conditions of the present or next examples. The extracted results of sandwich beam under non-uniform load based on the CTM are compared with those obtained based on the finite element method using the ABAQUS software. In this regard, the sandwich beam results with axial FG core are extracted based on the 3D theory of elasticity from ABAQUS software. To enhance accuracy of the results, C3D20R 20-node quadratic brick elements are used. In Fig. 2, discretization of the sandwich beam is shown and 153600 elements are employed in discretization of the beam.

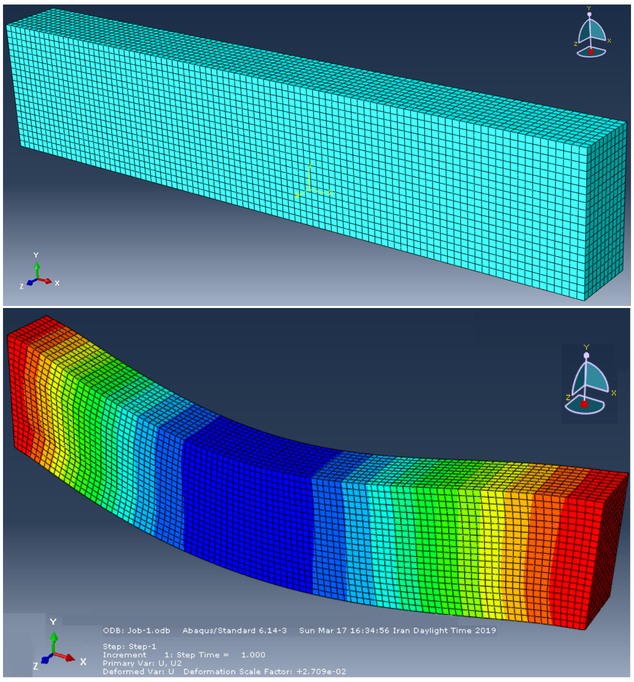

Fig. 2. Three-dimensional modeling of beam using ABAQUS software.

Results of transverse deflections of sandwich beam with homogeneous and axial FG core are presented in Fig. 3. The results of FG sandwich beam based on the considered variation of the material properties in the axial direction is different from the results of homogeneous sandwich beam and the lateral deflections of the plate with axial FG core is higher than the homogeneous ones, due to the lower rigidity. It can be observed that the present results are in good agreement with the results of the FEM. Also, based on the imposed non-uniform load and material properties distribution of FG sandwich beam, the maximum lateral deflection location moves to the left side of the beam and it does not occur at the middle point of the beam.

Table 1
Effects of choosing different number of terms (N) in the finite series of the solution on results of transverse deflection of FG sandwich beam.

X \ N	2	5	10	15	18	20
-1	0	0	0	0	0	0
-0.8	-0.5324	-2.036	-1.8898	-1.8815	-1.8815	-1.8815
-0.6	-0.9465	-4.9501	-3.6511	-3.6653	-3.6653	-3.6653
-0.4	-1.2420	-7.2659	-4.7116	-4.7111	-4.7111	-4.7111
-0.2	-1.4198	-8.2680	-4.9910	-4.9740	-4.9740	-4.9740
0	-1.4789	-7.8331	-4.5508	-4.5559	-4.5559	-4.5559
0.2	-1.4198	-6.2628	-3.6310	-3.6524	-3.6524	-3.6524
0.4	-1.2423	-4.1125	-2.5132	-2.5072	-2.5072	-2.5072
0.6	-0.9465	-2.0229	-1.3734	-1.3698	-1.3698	-1.3698
0.8	-0.5324	-0.5509	-0.4625	-0.4662	-0.4662	-0.4662
1	0	0	0	0	0	0

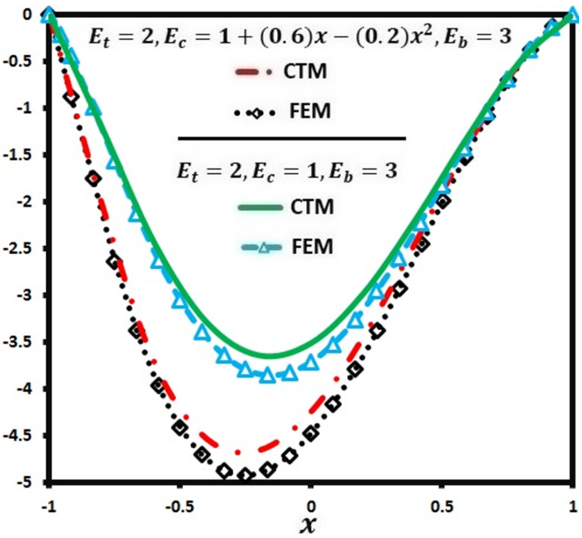

Fig. 3. The lateral deflections of the sandwich beams with homogeneous and axial FG core.

The transverse distributions of the in-plane displacement and stress of the sandwich beams with axial FG core are presented in Figs. 4 and 5 (at $x = -0.6$ and $x = 0.6$), respectively. It is observed that the present results are in good agreement with the extracted results using the ABAQUS software. The results are obtained based on a 2D sandwich plate theory (the layerwise theory) and the finite element results of the ABAQUS software are extracted based on the 3D-elacticity theory, so little difference is expected in the comparisons.

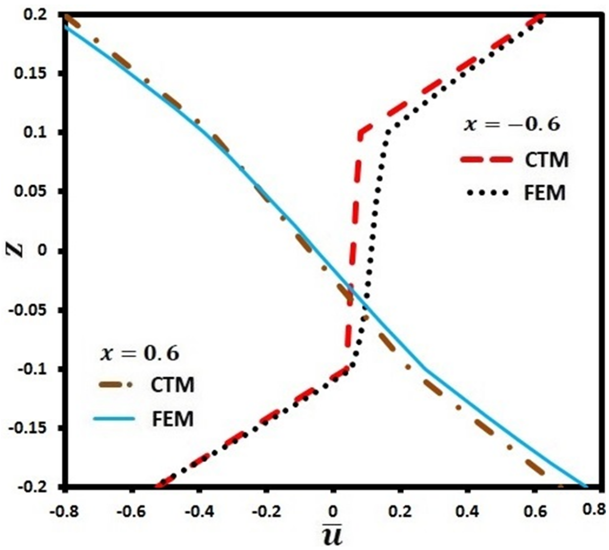

Fig. 4. The transverse variations of the in-plane displacement of the FG sandwich beams.

Example 2. In this example, the results of the FGB porous sandwich beam are presented. To cover both the axial and transverse variations of core porosity, elastic moduli of the core is defined as: $E_c = 1-s(1+0.6x-0.2x^2)$. Two different patterns for transverse variations of porosity (including uniform $s = s_0$ and non-uniform $s = s_0 \cos\left[\left(\frac{\pi}{2}\right)\frac{z}{h_c} + \left(\frac{\pi}{4}\right)\right]$ distributions) are considered. The lateral deflections of the FGB porous sandwich beams for four values of the porosity parameter: $s_0 = 0.1, 0.2, 0.3, 0.4$ are presented in Fig. 6. It is observed that increasing the porosity of sandwich beam leads to an increase in the lateral deflections, due to a decrease in the beam rigidity.

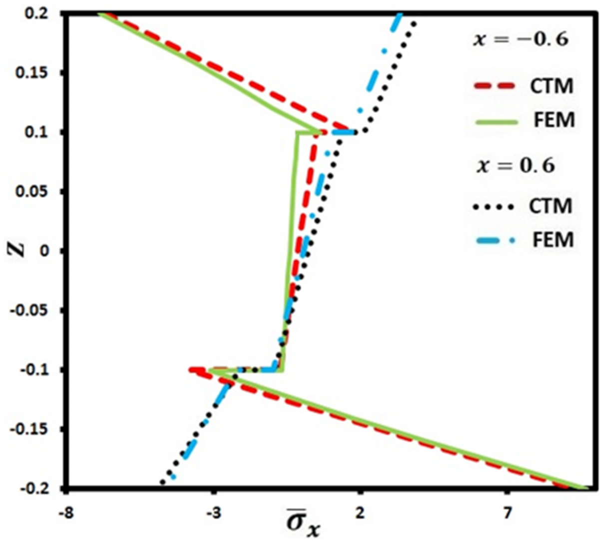

Fig. 5. The through-the-thickness variations of the in-plane stress of the FG sandwich beams.

The transverse variations of the in-plane displacement and stress at $x = 0.6$ are plotted in Figs. 7 and 8, respectively. It can be seen from Fig. 7 (also from Fig. 4), the local rotations of each layer are different, and thus the traditional equivalent plate theories cannot predict the transverse variations of the in-plane displacement of sandwich panels with various material properties of the layers. The top face sheet is stiffer than the bottom face sheet, and therefore the larger in-plane stresses have occurred in the bottom face sheet. It can be observed that increases in the porosity parameter of FGB porous core reduces the resulting in-plane displacement and the changes in the core displacements are more significant. Fig. 8 shows that increases in the porosity parameter (s_0) reduced the in-plane stress of core and face sheet.

Example 3. In this example, FGB porous sandwich beam resting on the Winkler/Pasternak foundation under non-uniform load is analyzed. The effects of the Winkler/Pasternak foundation on the lateral deflections of the FGB sandwich beams are shown in Fig. 9. As expected, increasing the Winkler/Pasternak foundation reduces the lateral deflection of FGB porous sandwich beam. The transverse variations of the in-plane displacement and the stress of FGB porous sandwich beam for different values of k_w and k_s are presented in Figs. 10 and 11, respectively. It can be seen that increases in the rigidity of the Winkler/Pasternak foundation reduces the resulting in-plane displacement and stress.

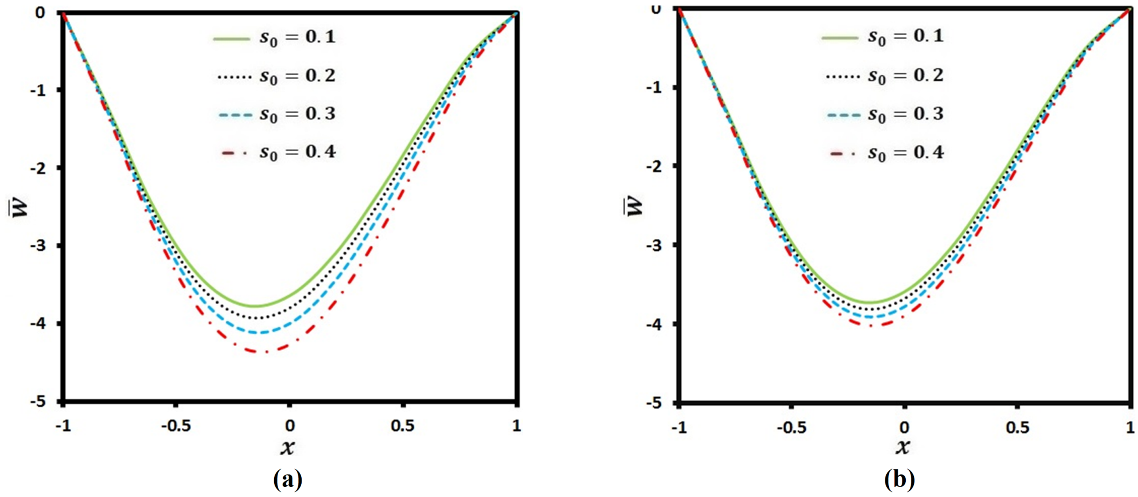

Fig. 6. The lateral deflections of FGB porous sandwich beam, a) Pattern A: $s = s_0$ and b) Pattern B: $s = s_0 \cos\left[\left(\frac{\pi}{2}\right)\frac{z}{h_c} + \left(\frac{\pi}{4}\right)\right]$.

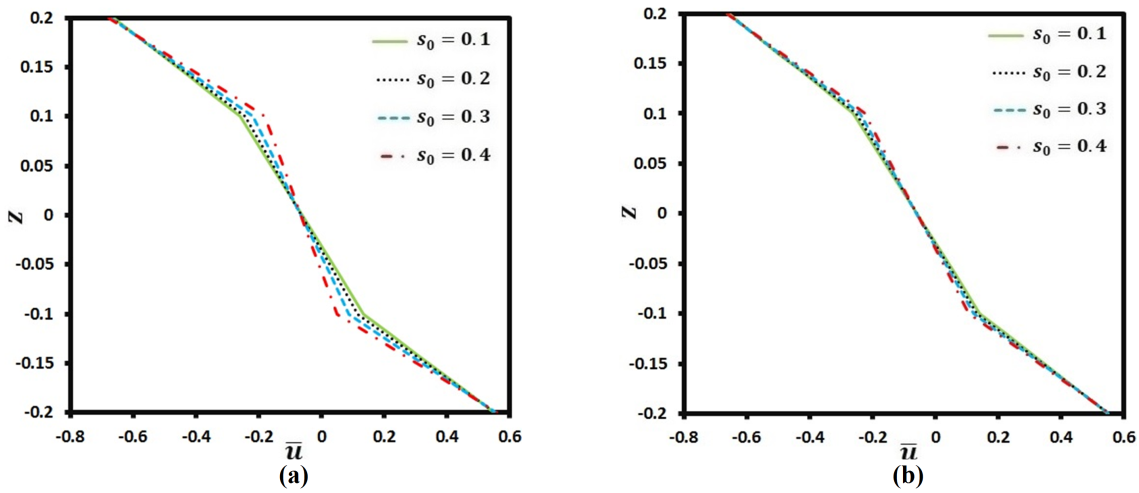

Fig. 7. The transverse variations of the in-plane displacement of FGB porous sandwich beam, a) Pattern A: $s = s_0$ and b) Pattern B: $s = s_0 \cos\left[\left(\frac{\pi}{2}\right)\frac{z}{h_c} + \left(\frac{\pi}{4}\right)\right]$.

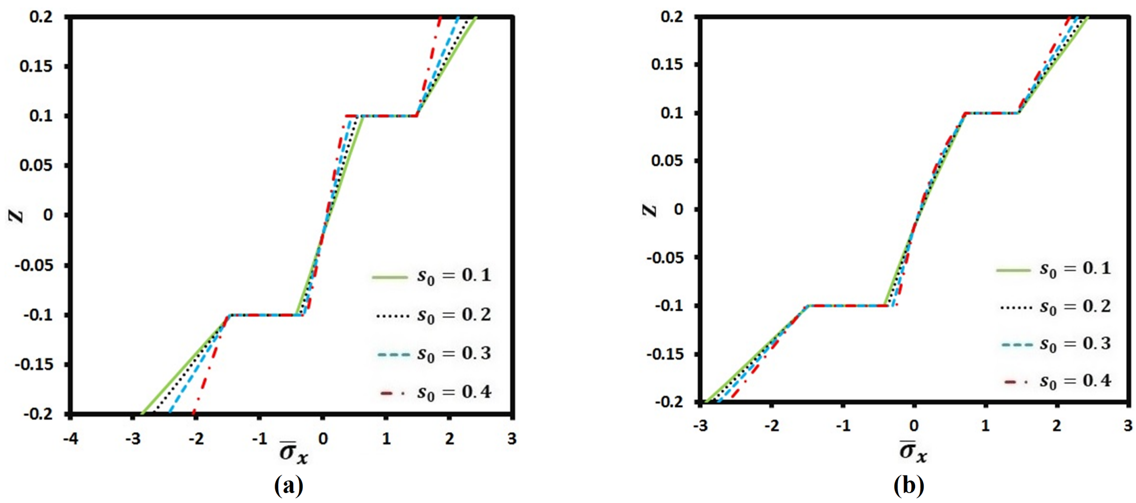

Fig. 8. The through-the-thickness distribution of the in-plane stress of FGB porous sandwich beam, a) Pattern A: $s = s_0$ and b) Pattern B: $s = s_0 \cos\left[\left(\frac{\pi}{2}\right)\frac{z}{h_c} + \left(\frac{\pi}{4}\right)\right]$.

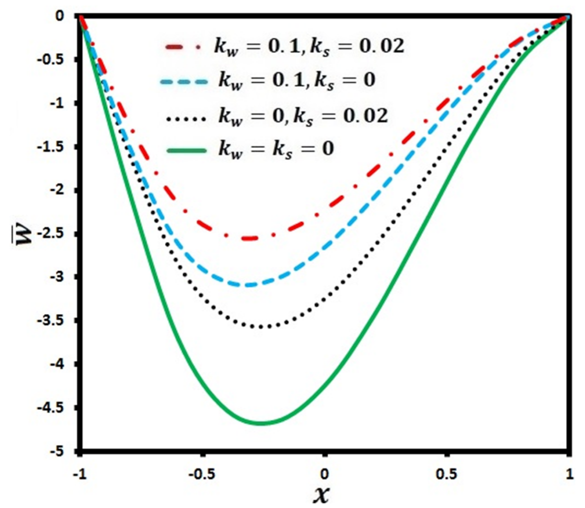

Fig. 9. Effects of Winkler/Pasternak foundation on the lateral deflection of the FGB sandwich beams.

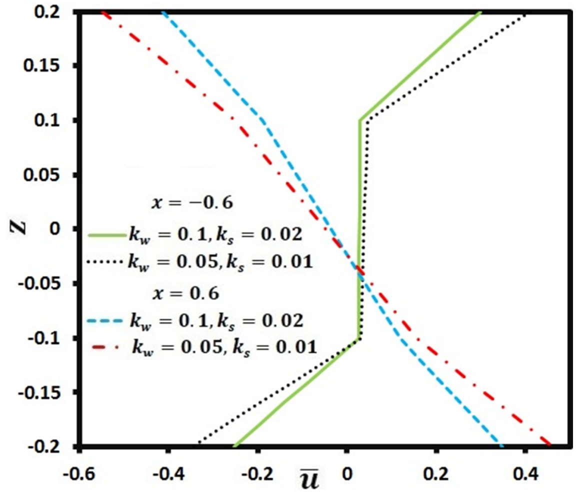

Fig. 10. Effects of Winkler/Pasternak foundation on the in-plane displacement of the FGB sandwich beams.

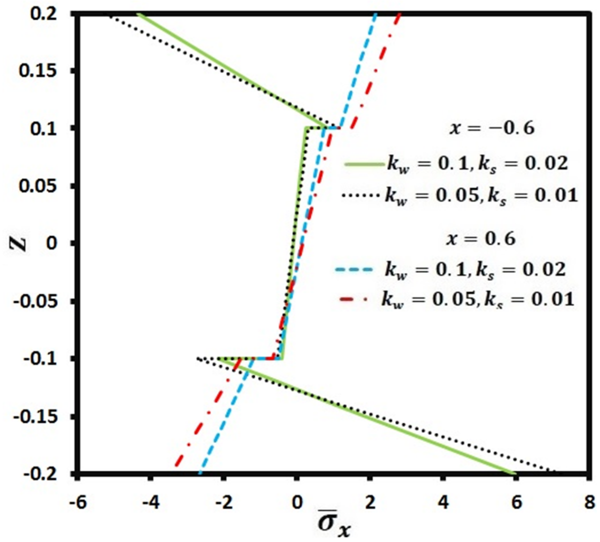

Fig. 11. Effects of Winkler/Pasternak foundation on the in-plane stress of the FGB sandwich beams.

Example 4. In-plane stress analyses of FGB porous sandwich beam in hygrothermal environment are conducted in this example. To extract more general results, asymmetric elastic moduli of the core is considered as:

$$E_c = 1 - 0.3\cos\left[\left(\frac{\pi}{2}\right)\frac{z}{h_c} + \left(\frac{\pi}{4}\right)\right](1 + 0.6x - 0.2x^2)$$

The transverse variations of the in-plane stress of the FGB porous sandwich beam for different values of hygrothermal parameters at $x = -0.6$ and $x = 0.6$, are depicted in Fig. 12. Due to the same effects of the thermal and moisture absorption expressions on the sandwich beam behavior, results are derived for various magnitudes of the $\Delta(TC) = (\alpha^{(c)}\Delta T + \beta^{(c)}\Delta C)$.

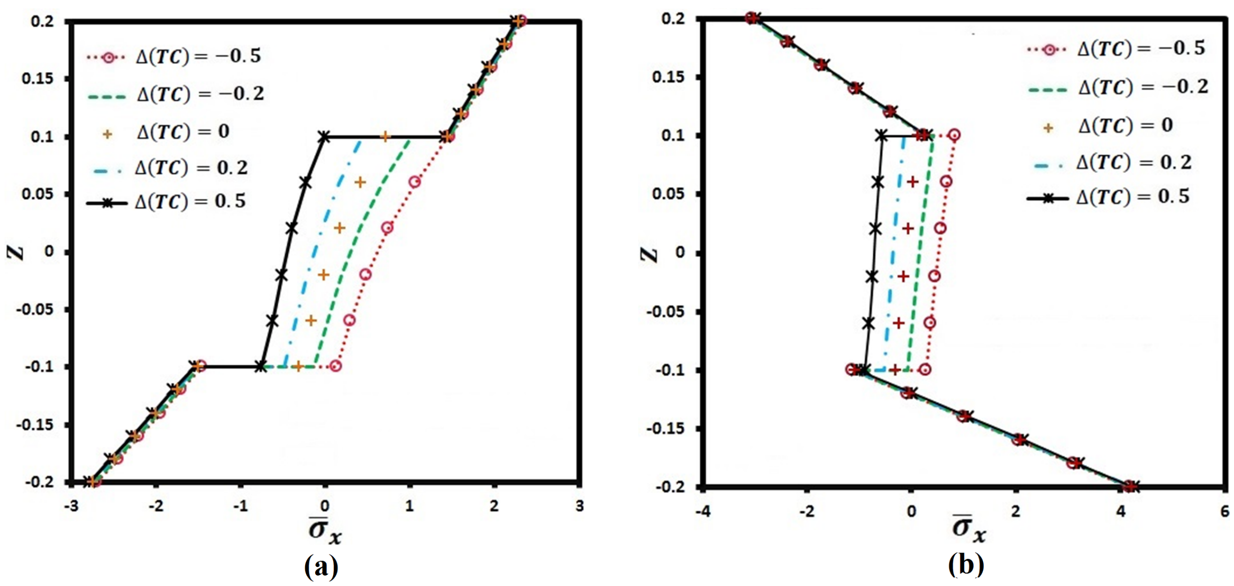

Fig. 12. The through-the-thickness variations of the in-plane stress of FGB porous sandwich beam at a) $x = 0.6$ and b) $x = -0.6$.

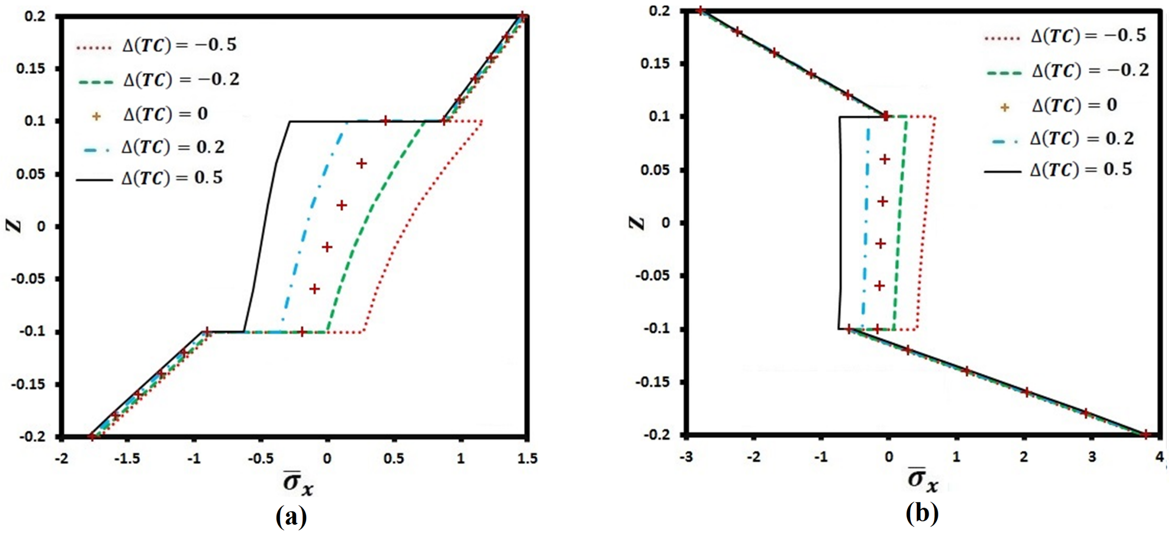

Fig. 13. The through-the-thickness variations of the in-plane stress of FGB porous sandwich beam under Winkler/Pasternak foundation at a) $x = 0.6$ and b) $x = -0.6$.

Results are presented for the five magnitudes as: $\Delta(TC) = -0.5, -0.2, 0, 0.2, 0.5$. Also, the results of the FGB porous sandwich beam under Winkler/Pasternak foundation ($k_w = 0.1$, $k_s = 0.02$) are shown in Fig. 13. The results show that due to the hygrothermal effects, the changes in the core are significant. It is obvious that by increasing the temperature gradients and moisture contents ($\Delta(TC)$) from -0.5 to 0.5, the in-plane stress of the core change from tensile stress to compressive stress.

It may lead to increased or decreased jumps at the interfaces between face sheets and core. For example, it can be observed from Fig. 13a that increasing the temperature gradients and moisture contents lead to increases in the jumps at the interfaces between top face sheet and core, and consequently decreases the jumps at the interfaces between bottom face sheet and core. However, the curve slopes are less sensitive to the hygrothermal loads.

6. Conclusion

For the first time, displacement and stress analysis of the bi-directional functionally graded (BDFG) porous sandwich beams are examined by using the Chebyshev tau method. The analyses are performed using the layerwise theory rather than the traditional equivalent single-layer theories whose results may not be reliable for the sandwich plates, in the majority of the general cases. Based on the presented analyses:

- Sandwich beams under non-uniform load can be analyzed.
- The material properties of each layer of sandwich beam can be varied continuously in the axial and thickness directions.
- The material properties can be affected by the variation of temperature and moisture.
- The effects of Winkler/Pasternak foundation on the sandwich beam can be examined.

References

[1] H. Niknam, A. Fallah, M.M. Aghdam, Nonlinear bending of functionally graded tapered beams subjected to thermal and mechanical loading, Int. J. Non-Linear Mech., 65 (2014) 141-147.

[2] S.R. Li, R.C. Batra, Relations between buckling loads of functionally graded Timoshenko and homogeneous euler-bernoulli beams, Compos. Struct., 95 (2013) 5-9.

[3] Y. Huang, X.F. Li, A new approach for free vibration of axially functionally graded beams with non-uniform cross-section, J. Sound Vib., 329(11) (2010) 2291-2303.

[4] Y. Huang, L.E. Yang, Q.Z. Luo, Free vibration of axially functionally graded Timoshenko beams with non-uniform cross-section, Compos. Part B: Eng., 45(1) (2013) 1493-1498.

[5] C.F. Lu, W.Q. Chen, R.Q. Xu, C.W. Lim, Semi-analytical elasticity solutions for bi-directional functionally graded beams, Int. J. Solids Struct., 45(1) (2008) 258-275.

[6] H. Deng, W. Cheng, Dynamic characteristics analysis of bi-directional functionally graded Timoshenko beams, Compos. Struct., 141 (2016) 253-263.

[7] Z.H. Wang, X.H. Wang, G.D. Xu, S. Cheng, T. Zeng, Free vibration of two-directional functionally graded beams, Compos. Struct., 135 (2016) 191-198.

[8] X. Chen, Y. Lu, Y. Li, Free vibration, Buckling and dynamic stability of bi-directional FG microbeam with a variable length scale parameter embedded in elastic medium, Appl. Math. Modell., 67 (2019) 430-448.

[9] X. Chen, X. Zhang, Y. Lu, Y. Li, Static and dynamic analysis of the postbuckling of bi-directional functionally graded material microbeams, Int. J. Mech. Sci., 151 (2019) 424-443.

[10] M. Simsek, Buckling of Timoshenko beams composed of two-dimensional functionally graded material (2D-FGM) having different boundary conditions, Compos. Struct., 149 (2016) 304-314.

[11] M. Simsek, Bi-directional functionally graded materials (BDFGMs) for free and forced vibration of Timoshenko beams with various boundary conditions, Compos. Struct., 133 (2015) 968-978.

[12] J. Li, Y. Guan, G. Wang, G. Zhao, J. Lin, H. Naceur, D. Coutellier, Meshless modeling of bending behavior of bi-directional functionally graded beam structures, Compos. Part B: Eng., 155 (2018) 104-111.

[13] S. Rajasekaran, H. Bakhshi Khaniki, Size-dependent forced vibration of non-uniform bi-directional functionally graded beams embedded in variable elastic environment carrying a moving harmonic mass, Appl. Math. Modell., 72 (2019) 129-154.

[14] T.T. Nguyen, J. Lee, Interactive geometric interpretation and static analysis of thin-walled bi-directional functionally graded beams, Compos. Struct., 191 (2018) 1-11.

[15] J. Fariborz, R.C. Batra, Free vibration of bi-directional functionally graded material circular beams using shear deformation theory employing logarithmic function of radius, Compos. Struct., 210 (2019) 217-230.

[16] A. Karamanli, Free vibration analysis of two directional functionally graded beams using a third order shear deformation theory, Compos. Struct., 189 (2018) 127-136.

[17] A. Pydah, A. Sabale, Static analysis of bi-directional functionally graded curved beams, Compos. Struct., 160 (2017) 867-876.

[18] J. Lei, Y. He, ZH. Li, S. Guo, D. Liu, Postbuckling analysis of bi-directional functionally graded imperfect beams based on a novel third-order shear deformation theory, Compos. Struct., 209 (2019) 811-829.

[19] M.M. Alipour, M. Shariyat, Stress analysis of two-directional FGM moderately thick constrained circular plates with non-uniform load and substrate stiffness distributions, J. Solid Mech., 2(4) (2010) 316-331.

[20] M.M. Alipour, M. Shariyat, A power series solution for free vibration of variable thickness Mindlin circular plates with two-directional material heterogeneity and elastic foundations, J. Solid Mech., 3(2) (2011) 183-197.

[21] C.I. Gheorghiu, Spectral Methods for Differential Problems, Tiberiu Popoviciu, Institute of Numerical Analysis, Cluj-Napoca Publisher, Romania, (2007).

[22] M. Shariyat, A.A. Jafari, M.M. Alipour, Investigation of the thickness variability and material heterogeneity effects on free vibration of the viscoelastic circular plates, Acta Mech. Solida Sin., 26(1) (2013) 83-98.

[23] C. Lanczos, Applied Analysis, Prentice-Hall, Englewood Cliffs, New Jersey, (1956) 464-517.

[24] D. Johnson, Chebyshev Polynomials in the Spectral Tau Method and Applications to Eigenvalue Problems, University of Florida Gainesville Publisher, Florida, (1996).

[25] S. Etehadi, M. Botshekanan Dehkordi, Effect of axial stresses of the core on the free vibration response of a sandwich beam with FG carbon nanotube faces and stiff and flexible cores, J. Stress Anal., 3(2) (2019) 1-14.

[26] M. Shaban, Elasticity solution for static analysis of sandwich structures with sinusoidal corrugated cores, J. Stress Anal., 1(1) (2016) 23-31.

[27] H.I. Siyyam, M.I. Syam, An accurate solution of the Poisson equation by the Chebyshev-Tau method, J. Comput. Appl. Math., 85(1) (1997) 1-10.

[28] M.R. Ahmadi, H. Adibi, The Chebyshev Tau technique for the solution of Laplace's equation, Appl. Math. Comput., 184(2) (2007) 895-900.

[29] A. Saadatmandi, M. Dehghan, Numerical solution of hyperbolic telegraph equation using the Chebyshev Tau method, Numer. Methods Partial Differ., 26(1) (2010) 239-252.

[30] H. Wang, An efficient Chebyshev-Tau spectral method for Ginzburg-Landau-Schrödinger Equations, Comput. Phys. Commun., 181(2) (2010) 325-340.

[31] M. Saravi, On the clenshaw method for solving linear ordinary differential equations, Am. J. Comput. Appl. Math., 1(2) (2011) 74-77.

[32] E. Carrera, Theories and finite elements for multilayered, anisotropic, composite plates and shells, Arch. Comput. Meth. Engng., 9(2) (2002) 87-140.

[33] E. Carrera, S. Brischetto, A survey with numerical assessment of classical and refined theories for the analysis of sandwich plates, Appl. Mech. Rev., 62(1) (2009) 010803.

[34] M.M. Alipour, M Shariyat, Analytical zigzag-elasticity transient and forced dynamic stress and displacement response prediction of the annular FGM sandwich plates, Compos. Struct., 106 (2013) 426-445.

[35] M.M. Alipour, A novel economical analytical method for bending and stress analysis of functionally graded sandwich circular plates with general elastic edge conditions, subjected to various, Compos. Part B: Eng., 95 (2016) 48-63.

[36] M.M. Alipour, M. Shariyat, Analytical layerwise stress and deformation analysis of laminated composite plates with arbitrary shapes of interfacial imperfections and discontinuous lateral deflections, Compos. Struct., 200 (2018) 88-102.

[37] M.M. Alipour, Effects of elastically restrained edges on FG sandwich annular plates by using a novel solution procedure based on layerwise formulation, Arch. Civ. Mech. Eng., 16(4) (2016) 678-694.

[38] J.C. Mason, D.C. Handscomb, Chebyshev Polynomials, Chapman and Hall/CRC Publisher, (2003).

[39] D.R. Gardner, S.A. Trogdon, R.W. Douglass, A modified tau spectral method that eliminates spurious eigenvalues, J. Comput. Phys., 80(1) (1989) 137-167.

[40] L. Fox, Chebyshev methods for ordinary differential equations, Comput. J., 4(4) (1962) 318-331.

[41] D. Gottlieb, S.A. Orszag, Numerical Analysis of Spectral Methods, SIAM Publisher, Philadelphia, (1977).

[42] W. Rudin, Real and Complex Analysis, McGraw-Hill, (1987).

[43] C. Canuto, M.Y. Hussaini, A.M. Quarteroni, T.H.A.J. Zang, Spectral Methods in Fluid Dynamics, Springer Series in Computational Physics, Springer-Verlag Publisher, (1988).